Poultry Science®

TMT-based quantitative proteomic analysis unveils uterine fluid difference in hens producing normal and pimpled eggs

Lina Song, Kaiqi Weng, Qiang Bao, Jia Wu, Yang Zhang, Qi Xu, and Yu Zhang[1]

Jiangsu Key Laboratory for Animal Genetic, Breeding and Molecular Design, Yangzhou University, Yangzhou, Jiangsu, China

ABSTRACT Eggshell is a crucial indicator of egg quality. Pimpled eggs (**PE**) a type of eggshell defect are characterized by low eggshell strength, leading to substantial financial losses. Eggshell formation occurs in the uterine fluid (**UF**), which contains the required ions and matrix proteins However, the underlying mechanisms of PE formation remain poorly understood. In this study, we analyzed the egg quality of PE, and normal eggs (**NE**) by examining the differences in UF from hens producing PE and NE ($n = 6$ each). This 2-wk-long assessment involved histomorphological and proteomics analyses. The results showed that NE had better eggshell quality compared to PE, and the uterus structure in PE hens was conducive to the formation of PE. Using quantitative proteomic analysis, we identified 68 differential abundance proteins (**DAPs**) in the UF of PE hens, including 9 key proteins related to ion transport, protein synthesis and folding, and immunity. Downregulation of CALM1 and SCNN1G proteins in PE hens might have negatively affected the calcium signaling pathway, decreasing the calcium amount in UF. Additionally, the PHB1 and TSN proteins may affect eggshell formation by regulating immune responses. Taken together, our results provide insights into the mechanism of PE production, with potential applications for enhancing eggshell quality.

Key words: chicken, eggshell quality, pimpled eggs, proteomics

2023 Poultry Science 102:103081
https://doi.org/10.1016/j.psj.2023.103081

INTRODUCTION

Chicken eggs, mainly composed of shell (including membrane), albumen, and yolk, are considered a significant source of animal protein for humans (Ahmed et al., 2021; Pan et al., 2021; Zhang et al., 2022). Eggshell provides mechanical protection to egg contents while ensuring gas exchange and calcium for the developing embryo (Hahn et al., 2017). Eggshell, an important indicator of egg quality, is closely monitored in the poultry industry to prevent financial losses from damage during transportation and storage (Wang et al., 2021). Pimpled eggs (**PE**), however, are a defect characterized by the presence of extra-calcified granules on either end of the eggshell. PE have weaker shells and are more susceptible to breaking compared to normal eggs (**NE**) under the same conditions (Liu et al., 2017a,b). The strength of the eggshell weakens further if the pimples are removed from the surface of PE (Roland Sr et al., 1975). This causes the leakage of egg contents, raising concerns about food quality and safety.

The process of egg formation in the ovaries and fallopian tubes takes about 24 to 25 h in hens, with the eggshell formation being the longest stage, requiring about 20 h in the uterus, while the needed substances are derived from uterine fluid (**UF**) (Wasserman et al., 1991). The eggshells are a special bioceramic material consisting of highly ordered calcification layers containing 3.5% organic matrix proteins and 95% calcium carbonate ($\mathbf{CaCO_3}$) (Marie et al., 2014). Scanning electron microscopy of the eggshell consists of different layers in its ultrastructure, from inside to outside: eggshell membranes, mammillary layer, palisade layer, vertical crystal layer, and cuticle. For study purposes, the eggshell can be divided into 2 distinct layers, mammillary and effective layers (Nys et al., 2010; Hincke et al., 2012). The entire process of eggshell formation involves 3 distinct stages: the incipient stage (lasting about 5 h) involving the formation of the mammillary layer, the linear calcification stage (taking about 12 h) involving the formation of the palisade layer, and the termination stage (lasting about 1.5 h) involving pigmentation (Nys et al., 2004; Marie et al., 2015). The mineralization of the mammillary and palisade layers is the most critical aspect of eggshell formation, and, at that time, conditions of the uterus

Received June 19, 2023.
Accepted August 27, 2023.

[1]Corresponding author: yuzhang@yzu.edu.cn

directly affect the quality of the eggshell. The $CaCO_3$ precursors during mineralization mainly originate from carbon dioxide ($\mathbf{CO_2}$) and calcium ions ($\mathbf{Ca^{2+}}$) in the blood (Zhang et al., 2017). The uterine gland cells transfer CO_2 and Ca^{2+} to the UF. Endometrium atrophy, which can be a result of an increase in uterus cilia length or decreased secretion of gonadal hormones, can reduce the regenerative capacity of the endometrial cells, declining the function of different ion channels in the uterine gland cells (Huntley and Holder, 1978; Woudstra and Thomson, 2002). This may particularly cause abnormal transport of calcium ions, resulting in disordered $CaCO_3$ deposition and eggshell defects such as speckles, cracks, and pimples (Zhu et al., 2019). Previous research suggests that genetic factors are the main causes of eggshell defects (Wolc et al., 2012). However, the mechanism of PE production remains unclear. Searching for specific proteins in the uterus that regulate eggshell quality can help us understand the mechanism of PE production with potential applications for improving eggshell quality in subsequent generations of layer-breeding stock .

UF serves as a medium between eggshell and hen, regulating eggshell calcification. Particularly, during the rapid deposition stage, UF may have a closer relationship with eggshell quality. Some previous proteomic studies have examined the eggshells of PE and NE. In this study, we used 160-day-old Langshan laying hens, to examine the difference in uterine tissue and UF of NE- and PE-producing hens. The quality of PE and NE was also examined. Furthermore, we used TMT-based quantitative proteomics to detect differential proteins in the UF of hens producing PE and NE. Our data uncover key factors involved in the production of PE.

MATERIALS AND METHODS

Birds Management

All animal studies protocols were approved by the institutional animal care committee of Yangzhou University (Jiangsu, China). In this study, we used the Langshan laying hens (*Gallus gallus*) that were raised in the Rudong County Langshan chickens Breeding Farm (Nantong, Jiangsu, China). In total, three thousand 160-day-old Langshan laying hens were caged individually and subjected to a photoperiod of 16-h light and 8-h darkness. The feed formula (Supplementary Table S1) was prepared according to NRC recommendations (1994).

Selection of Hens and Sample Collection

All the eggs (NE, PE, broken and cracked eggs, etc.) were collected, counted, and recorded during the entire laying period daily. In addition, the PE production rate per day was calculated. The entire egg-laying process was divided into 3 distinct stages based on the age of laying of hens: the early stage (135−176 d), the middle stage (177−419 d), and the later stage (420−448 d). During the 2-wk egg collection period, the cages containing NE and PE (the eggshell area had >40% pimples) were recorded (Figure 2). From the laying hens, 6 laying hens that continuously laid NE were selected as the NE group and 6 laying hens that continuously laid PE were selected as the PE group. Six hens from each group were sacrificed by cervical dislocation, and their uteri were collected for uterine structure analysis. Subsequently, the uterus was cut open with sterile scissors, to collect the UF, which was rapidly frozen in liquid nitrogen and stored at −80°C until further use.

Examination of Egg Traits and Eggshell Ultrastructure

Six eggs per group were collected, and all measurements were made on the day of sampling. Egg weight, yolk weight, yolk color, albumen height, and haugh unit were estimated using an egg analyzer (EMT-5200, Robotmation, Co., Ltd., Tokyo, Japan). The egg shape index (length/width) was calculated using a caliper. Eggshell breaking strength was determined using an Eggshell Force Gauge (EFG-0503, Robotmation Co., Ltd., Tokyo, Japan). Eggshell thickness was measured using a dial pipe gauge (EFG-1061A, Robotmation Co., Ltd., Tokyo, Japan). The eggshell ultrastructures were examined under a scanning electron microscope (JSM-6390LV, JEOL Ltd., Tokyo, Japan).

Hematoxylin-Eosin Staining of Uterine

The uterine tissues were cut into sections and embedded in paraffin for 24 h. Thereafter, each section was subjected to hematoxylin-eosin (**HE**) staining. The ImageJ software (National Institutes of Health, Bethesda, MD) was used to examine the density of uterine glands.

Western Blotting

Proteins were extracted from the UF, and the total protein concentration was quantified using a BCA assay (Beyotime Biotechnology, Shanghai, China) following the manufacturer's instructions. The protein samples were denatured at 95°C for 5 min containing the 5 × loading buffer. The denatured protein sample was subjected to 10% SDS-PAGE and then proteins were transferred onto a PVDF membrane, following incubation with target primary antibodies: Calmodulin Antibody (CALM1, Abmart, Shanghai, China), PEBP1, PHB1, and GAPDH (ABclonal, Wuhan, China). Blot bands were visualized using the horseradish peroxidase-conjugated secondary antibodies and chemiluminescent substrate. Protein band intensities were quantified using the ImageJ software. The used antibodies were diluted according to their manufacturer's instructions.

Protein Extraction, Trypsin Digestion, and TMT Proteomic Labeling

To reduce the individual level variation, each group comprised 4 biological replicates ($n = 4$). In total, 8 UF

(4 UF/group) were suspended in lysis buffer (10 mM DTT, 8 M urea, and protease inhibitor). The corresponding suspensions were centrifuged for 20 min at 12,000 × *g* to collect the supernatants. The supernatant protein concentration was determined using Pierce BCA Protein Assay Kit (Thermo Fisher Scientific, Waltham, MA). Sample protein digestion was performed with trypsin according to the following FASP procedure (Wiśniewski et al., 2009). Briefly, 30 μL of the SDT buffer was introduced into each sample of protein (200 μg): the detergent from STD buffer, DTT, and other low-molecular-weight components were removed using repeated ultrafiltration against the UA buffer (pH 8.0). Hundred microliters of uric acid buffer contained 100 mM iodoacetamide to obstruct reduced cysteine residues during the sample incubation in the darkness for 30 min. The filters were washed thrice with 100 μL uric acid buffer, followed by twice washing with 100 μL 25 mM NH_4HCO_3 buffer. Eventually, trypsin was introduced at a 1:10 trypsin-to-protein mass ratio to digest protein suspensions at 37°C for more than 4 h, and the digested protein peptides were collected. After the trypsin digestion, samples were desalted by C18 cartridges (Sigma-Aldrich, St. Louis, MO), and then vacuum-dried. The peptides (100 μg) were reconstituted and processed using the TMT16plex Isobaric Label Reagent Set, as per the kit directions (Thermo Fisher Scientific, Waltham, MA).

HPLC Fractionation and LC-MS/MS Analyses

Peptide mixtures were fractionated by reverse-phase HPLC equipped with a Waters XBridge Peptide BEH C18 column. The mobile phase was made up of water, acetonitrile, and formic acid (at the proportion of A:100/0/0.1%; B:20/80/0.1%). The peptides were separated at a flow rate of 0.7 mL/min. Orbitrap Eclipse Tribrid mass spectrometer was used to analyze the fractionated peptides (Thermo Fisher Scientific). The Nanospray Flex Ion source had a voltage of 2.0 kV, and the temperature of the ion transfer tube was 320°C. The mass spectrometry (**MS**) data were collected using the mass spectrometer. The MS1 full scanning range was 350 to 1,800 m/z at a resolution of 120,000 (200 m/z). Regarding the second-stage mass spectrometry (**MS2**) scans, parent ions with the TOP 40 ionic strengths from the MS1 full scan were selected to be fragmented by high-energy collision dissociation at a resolution of 30,000 (200 m/z).

Protein Identification and Quantification

Proteome Discoverer (2.4.1.15) was used to quantitatively analyze the RAW files of mass spectra, and the database search analysis was carried out using the embedded SEQUEST and RefSeq human protein databases. The fixed modification method was used for the carbamidomethylation of cysteine (+57.02146 Da), while the variable modification involved the oxidation of methionine (+15.99492 Da). The MS tolerance was set at 20 ppm, with a fragment ions tolerance of ±0.05 Da. The used digestive enzyme was trypsin, and up to 2 missed cleavages were allowed. The reverse sequence decoy strategy was employed to control false positives, which were verified using the Percolator software. The false discovery rate (**FDR**) for protein and peptide matching (**PSMs**) was set to 0.01 (Subramanian et al., 2005). Background data errors were checked and corrected using the median method. Only the proteins containing at least one unique peptide were considered for subsequent quantitative and functional analyses.

Statistical and Bioinformatic Analysis

The difference in egg traits and other variables between NE and PE were compared using the paired sample *t* test in SPSS 25.0 software. All data were evaluated as mean ± standard error (**SE**), and those with a P value ≤0.05 were considered statistically significant. Proteins meeting the criteria of fold change (**FC**) >1.2 and $P \leq 0.05$ were deemed significantly different (differential abundance protein; **DAPs**). The Gene Ontology (**GO**) functional enrichment analysis (Ashburner et al., 2000) and the Kyoto Encyclopedia of Genes and Genomes (**KEGG**) pathway enrichment analysis (Kanehisa et al., 2004) were conducted using the Fisher's exact test and the list of differential proteins. Correlation analysis between DAPs was performed using the String database (Szklarczyk et al., 2019) and the network diagram was constructed using the igraph software.

RESULTS

Quantity and Eggshell Ultrastructure of NE and PE

In this study, the production rate of PE was significantly higher in the early stage of egg laying than in the middle and later stages of egg laying ($P < 0.05$) (Figure 1A). Egg quality and eggshell ultrastructure analysis revealed no significant differences in yolk color, albumen height, egg weight, eggshell strength, eggshell thickness, yolk weight, and haugh unit, and egg shape index between the PE and NE groups ($P > 0.05$) (Figure 1B). Figure 1C shows the cross-sectional image of the eggshell from PE and NE. The mammillary layer thickness (**MLT**), effective layer thickness (**ELT**), and mammillary knob width (**MKW**) were quantified to assess the differences in eggshell ultrastructure between the PE and NE groups (Figure 1D). The ELT of PE was apparently higher ($P < 0.05$) (Figure 1D), while the MLT, the effective layer ratio (**TELR**), mammillary layer ratio (**MLR**), and MKW were lower ($P < 0.05$) compared with NE (Figure 1D). These results indicated that the eggshell quality of NE was better than that of PE.

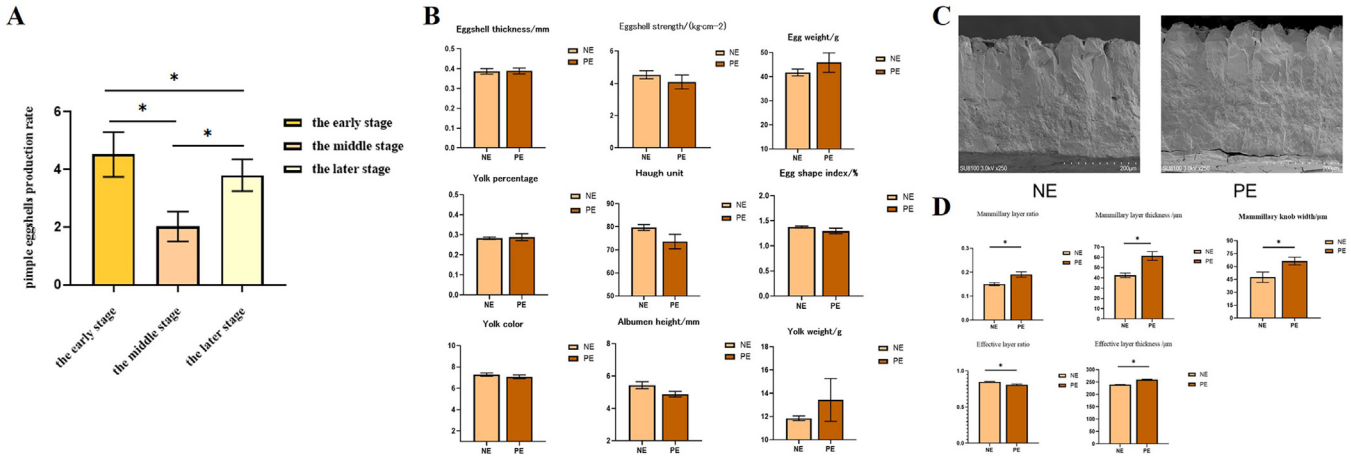

Figure 1. Analysis of pimpled eggs production rate, egg quality traits, and ultrastructure of eggshells. (A) Pimpled egg production rate at the early, middle, and later stages. (B) Comparison of egg quality traits of normal and pimpled eggs. (C) The transverse view of the eggshell ultrastructure of normal and pimpled eggs. (D) The parameters in eggshell ultrastructure of normal and pimpled eggs. Data are shown as mean ± standard deviation (SD).

Morphological and Histological Characteristics of Uteri

In the present study, we found that eggs were present in the uterus of both PE and NE hens. Histological observations found that uterine glands in the chicken uterine endometrium had a folded and branched tubular structure. However, the density of the uterine glands was significantly increased in PE hens compared with NE hens. Additionally, the uterus in the PE group showed a longer length and more complex folding of uterine glands compared with those from the NE group (Figure 2). This change in the uterine glands potentially increased the contact area between the uterus and egg, stimulating the uterus to secrete large amounts of UF in PE hens. Notably, the UF contains various ions and matrix proteins for eggshell formation such as HCO_3^-, H^+, Ca^{2+}, Ovocleidins-17, Ovocalyxins-32, etc. (Marie et al., 2014). Taken together, these results indicated that UF in the PE group had more matrix proteins and ions for eggshell formation than in the NE group. A comparison of UF proteomics among the 2 groups could reveal the DAPs participating in eggshell formation.

Proteomic Analysis of UF From Normal and Pimpled Eggshells Chickens

TMT-based quantitative proteomics of UF was performed to analyze the DAPs between the 2 groups of

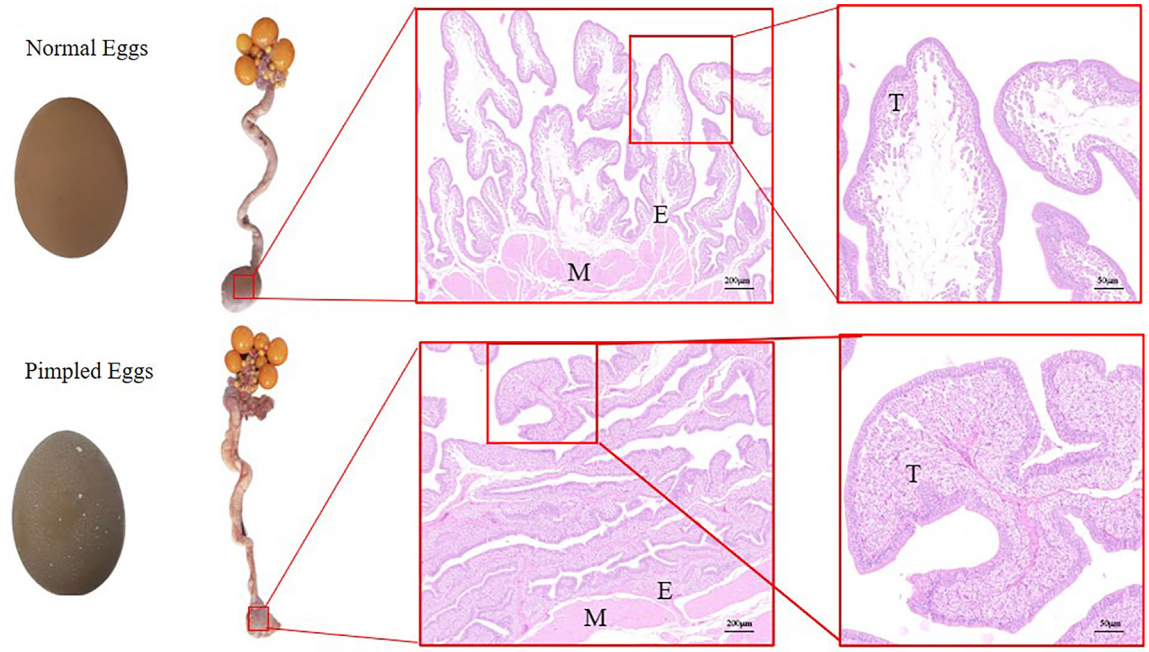

Figure 2. Egg specimens and chicken uterus morphology and histological characteristics. Hematoxylin and eosin staining of the uterus from normal and pimpled eggshells chickens, respectively. Magnification, 200×; Replications, 3. E: endometrium; M: myometrium; T: tubular gland cells. The black arrow indicates the endometrial glands.

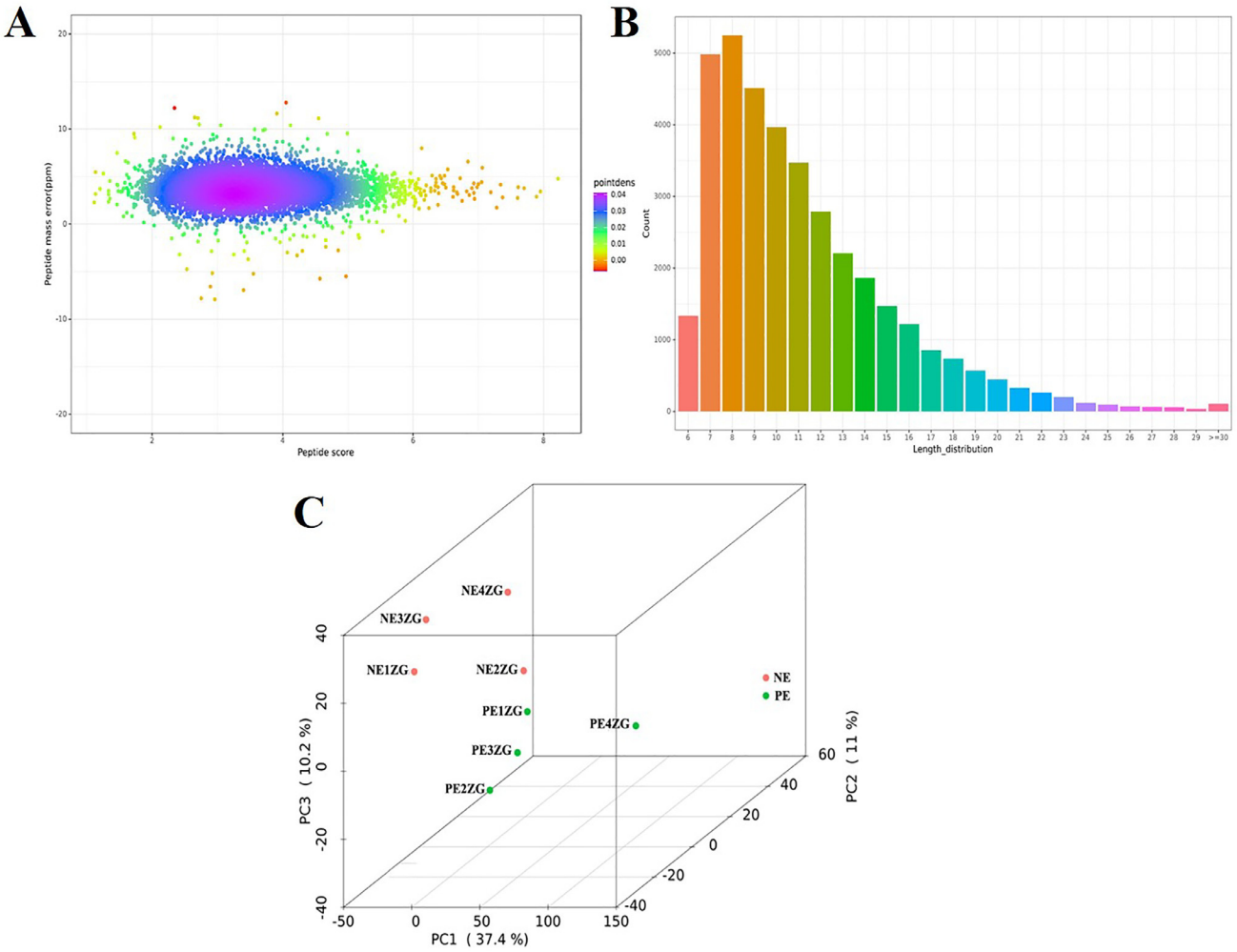

Figure 3. Proteomic quality control analysis. (A) Peptide's mass error. (B) Distribution and number of peptide fragments. (C) Three-dimensional principal component analysis (PCA) of 2 groups with 4 biological replicates.

hens. In the LC−MS/MS analysis, we observed the average peptides mass error was <20 ppm, indicating a good accuracy of the MS data (Figure 3A). Additionally, the length of peptides corresponding to most proteins identified by MS was between 8 and 35 amino acid residues (Figure 3B), indicating that sample preparation was of required standard with complete trypsin digestion. In total, 4,684 proteins were identified and quantified from the 2 groups, and most of the proteins were common to both groups. The 3-dimensional principal component analysis clearly distinguished 8 samples into 2 major categories, which are marked with different colors in Figure 3C, indicating the biological reproducibility of the samples.

DAPs Between Normal and Pimpled Eggshells Chicken

To examine the differences between the UFs of PE and NE hens, we identified DAPs based on the criteria of FC >1.2 and P value <0.05. In total, 68 DAPs including 24 upregulated and 44 downregulated proteins were identified in the PE group compared to the NE group (Figure 4A). Supplementary Table S2 provides detailed information about these DAPs. Subsequently, hierarchical clustering analysis was performed on DAPs to visualize the variations in protein abundance (Figure 4B). The expression patterns of DAPs were consistent within the sample groups, indicating substantial changes in protein expression levels only between the 2 groups.

Functional Enrichment Analysis of DAPs

To better understand the functional roles of DAPs, we performed GO enrichment, KEGG pathway, and protein-protein interaction network analyses. As shown in Figure 5A, the results of GO analysis were considered statistically significant at $P < 0.05$. GO enrichment analysis classified DAPs based on biological processes (**BPs**), molecular functions (**MFs**), and cellular components (**CCs**) modules. The BPs mainly include translation, B cell receptor signaling pathway, phagocytosis, ribosomal large subunit biogenesis and immune response. The CCs were the external side of plasma membrane, immunoglobulin complex (circulating), nucleosome, mitochondrial outer membrane, and

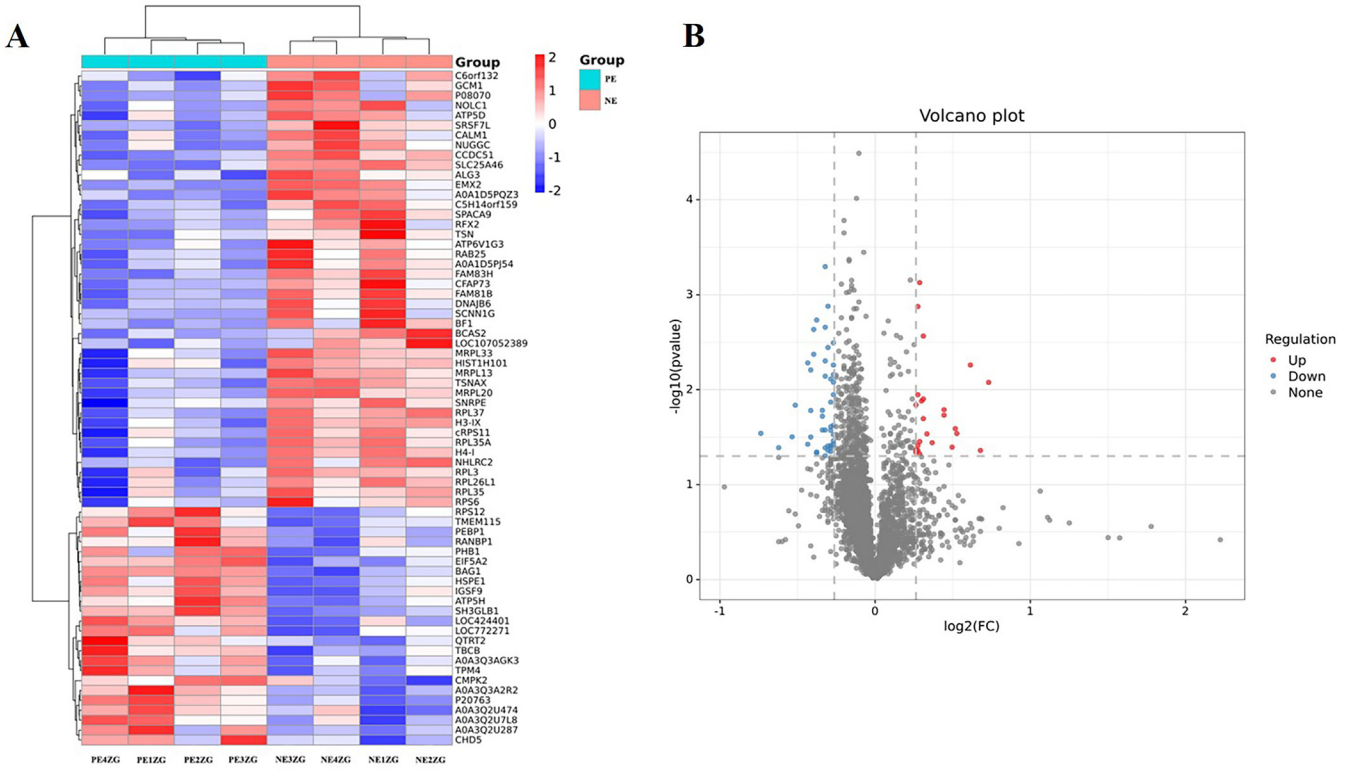

Figure 4. Identification and comparison of differential proteins. (A) Hierarchical clustering analysis of differential proteins in NE and PE group. *X*-axis displays analyzed samples, and *Y*-axis corresponds to differential proteins; red and blue indicate the high and lower levels, respectively. (B) Volcano plots of NE and PE groups. The fold change criteria were >1.2 with $P < 0.05$. *X*-axis displays the fold change of differential proteins (value of log2), and *Y*-axis corresponds to the *P* value (value of −log10). Gray represents proteins with insignificant differences, red indicates upregulated proteins, and blue corresponds to downregulated proteins.

ribosome. The key MFs were structural constituents of the ribosome, immunoglobulin receptor binding, antigen binding, and heat shock protein binding.

Additionally, the highly significant KEGG pathway terms related to DAPs were coronavirus disease, intestinal immune network for IgA production, ribosome, thermogenesis, and neutrophil extracellular trap formation (Figure 5B).

Using the STRING PPI database and igraph software, a protein-protein interaction network of DAPs was constructed (Figure 6). The largest cluster network was of the ribosomal proteins, the second largest was of the other proteins. The nodes in the PPI network represent the DAPs. The number of nodes that directly interact with a certain node denotes the degree of connectivity of that particular protein. In principle, the greater the protein connectivity, the more important the protein is in the network, indicating that this protein may be the hub stabilizing the protein network. To further identify the key proteins associated with eggshell formation, we analyzed and identified the top 10 proteins based on the degree of nodes in the PPI network. These proteins were mainly related to protein synthesis and folding-related functions.

Taken together, the results of GO, KEGG, and PPI network analyses suggested that the formation of pimpled eggshells in the UF of PE hens was regulated by proteins involved in the synthesis and folding of ribosomes-related proteins, immune process-related proteins and other proteins. Particularly, we validated 3 key protein antibodies, named CALM1, PEBP1, and PHB1, from the proteomic data by Western blotting, and the results showed that the expression levels of these proteins were consistent with the proteomics (Supplementary Figure S1).

Putative Proteins Were Potentially Implicated in the Formation of Pimpled Eggshells

To speculate on all proteins that might be associated with the formation of pimpled eggshells, each DAP was searched and analyzed in relevant databases (NCBI or UniProt) and literature. Ultimately, 9 of the 68 differential proteins, mainly related to ion transport, protein synthesis and folding, and immune-related functions, were found to be significant in the formation of eggshells. The functional description for these proteins is listed in Table 1.

DISCUSSION

The eggshell is the primary defense protecting eggs from microbes and is the most intuitive indicator for product selection by consumers. Pimpled eggshells, a cosmetic eggshell defect, are usually manifested as poor eggshell quality, reducing economic benefits to farmers.

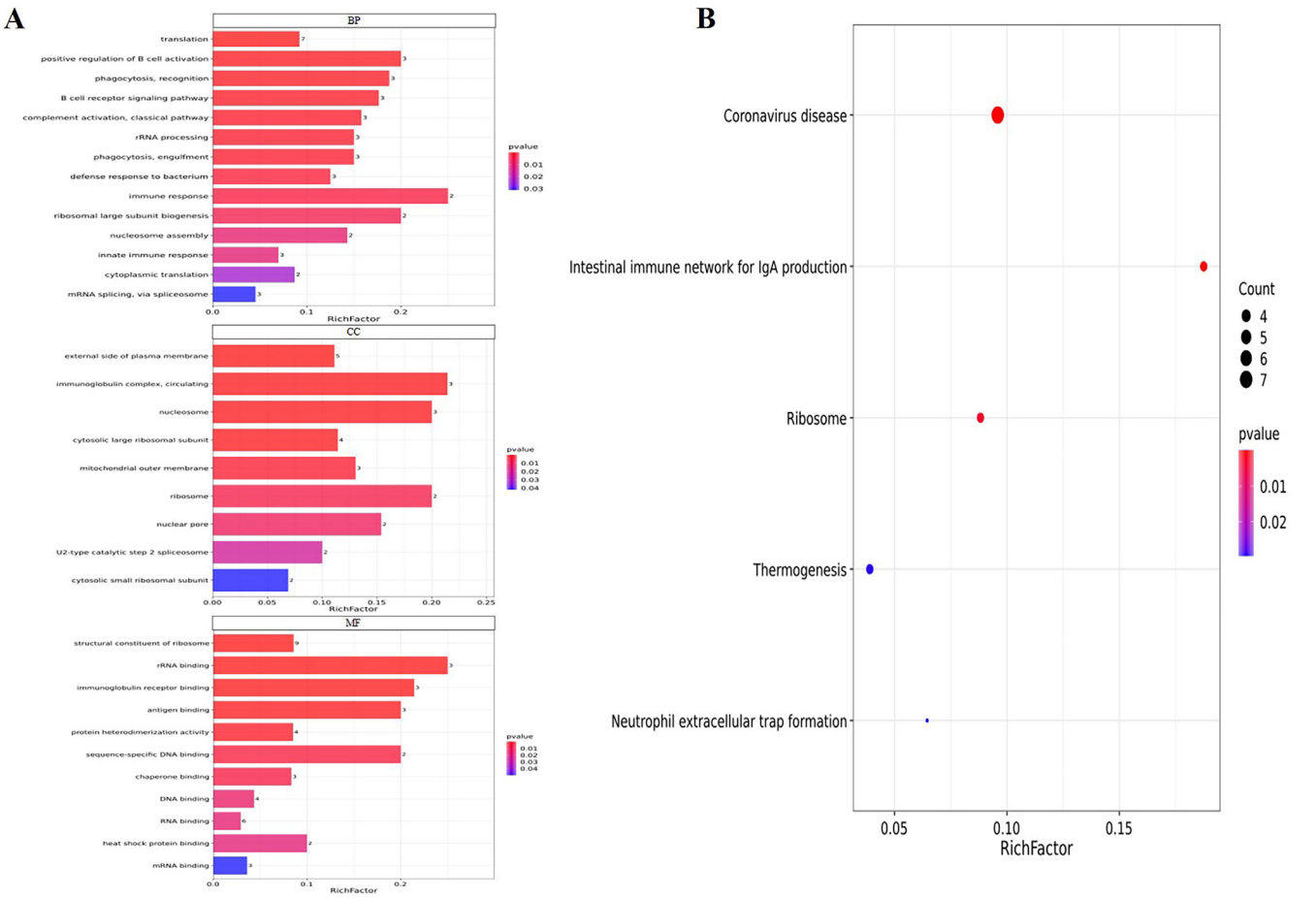

Figure 5. Gene Ontology and KEGG pathway analysis of differential proteins in normal and pimpled eggshells chicken uterine fluids. (A) The abscissa represents the enrichment factor, and the ordinate represents enriched GO terms. The colors in the figure correspond to the *P* value, and red indicates significant enrichment. The numbers in the figure indicate the number of differential proteins in the corresponding GO terms. BP, biological process; MF, molecular function; CC, cellular component. (B) The *X*-axis displays the enrichment factor, and *Y*-axis represents the significantly enriched KEGG pathways. Colors indicate the *P* value, and red indicates significant enrichment. The size of the point represents the number of differential proteins.

In this study, we first assessed and compared the egg quality traits of NE and PE. Notably, consistent with previous results (Liu et al., 2017b), the egg weight, yolk weight, yolk color, yolk percentage, albumen height, haugh unit, and egg shape index showed no significant differences between NE and PE. Fu et al. also studied the eggshell traits of eggs from 3 kinds of Muscovy ducks and reported no significant difference in egg weight, egg shape index, and eggshell thickness between PE and NE, which is consistent with our results (Fu et al., 2023). Though the eggshell strength of PE was lower than that of NE, the difference was not significant. However, the SEM ultrastructure analysis showed significant differences in the effective layer of PE and NE, which may be related to the breed of chicken. Notably, the eggs from Langshan chicken are much smaller compared to normal eggs, so both PE and NE from Langshan chicken can be subjected to a greater force. Meanwhile, in addition to nutritional, genetic, and environmental factors, eggshell quality is determined by its ultrastructure (Rodriguez-Navarro et al., 2002; Wolc et al., 2012). Previous ultrastructure studies have focused on both the palisade layer and the mammillary layer (Van Toledo et al., 1982; Brionne et al., 2014). Therefore, here, we observed the eggshell ultrastructure using a scanning electron microscope, and found that the MLT, MKW, and MLR were significantly lower in the PE group than

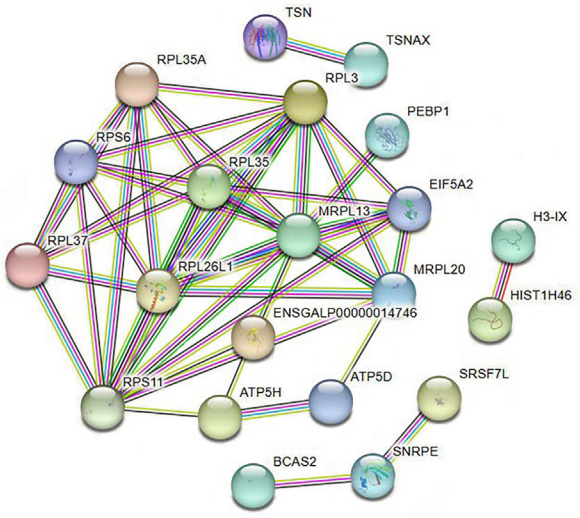

Figure 6. Protein-protein interaction networks of differential proteins in normal and pimpled eggshells chicken uterine fluids.

Table 1. Functional description of proteins potentially contributing to the formation of pimpled eggshells.

Functional class	Protein name (gene symbol)	Annotation
Ion transport related	Calmodulin-1 (*CALM1*)	Calcium-binding
	Amiloride-sensitive sodium channel subunit gamma (*SCNN1G*)	Sodium ion diffusion
Protein synthesis and folding	10 kDa heat shock protein (*HSPE1*)	Facilitates the correct folding of imported proteins
	DnaJ homolog subfamily B member 6 (*DNAJB6*)	Acts as a co-chaperone of HSP70, facilitates the correct folding of imported proteins
	Ribosomal protein L37 (*RPL37*)	responsible for the synthesis of protein
	60S ribosomal protein L35 (*RPL35*)	responsible for the synthesis of protein
	60S ribosomal protein L35a (*RPL35A*)	responsible for the synthesis of protein
Immune-related	Prohibitin1 (*PHB1*)	Protein with pleiotropic attributes, participation in immunization
	Translin (*TSN*)	Involving immunoglobulin /T-cell receptor gene segments

in the NE group. The mammillary layer of the eggshell consists of a mammillary knob (**MK**), the base of which is embedded in the eggshell membrane and connected to the eggshell membrane. The binding strength between the MK and the eggshell membrane affects the quality of eggshells (Nys et al., 2010; Athanasiadou et al., 2018). An increase in the width of MK decreases its density and the binding strength between the MK and the eggshell membrane, reducing eggshell strength (Dunn et al., 2012; Radwan, 2015). Besides, many studies have found that the change in MLT is closely related to the strength of eggshells (Gongruttananun, 2018). An increase in MLT decreases eggshell strength (Zhang et al., 2017), which is consistent with our results. We also found lower TELR in PE compared with NE. Some studies have demonstrated that the thickness of the effective layer can alter the mechanical characteristics of eggshells (Zhu et al., 2020). Zhang et al. found that lower eggshell strength was associated with lower decreasing TELR (Zhang et al., 2019). Taken together, the results of egg quality and eggshells ultrastructure analysis indicated that the eggshell quality of NE was better than that of PE.

Previous research has shown that eggshell formation in the uterus. During the formation of an eggshell, Ca^{2+} is transported into the UF by the uterine epithelial cells. Increased expression of calcium-binding proteins in uterine gland cells promotes calcium accumulation in the UF and thereby its growth on the surface of the eggshell, resulting in PE (Ebeid et al., 2012; Cheng and Ning, 2023). Therefore, in the present study, we compared the structure of the uterus of the NE- and PE-producing hens by HE staining. The results demonstrated that the number of uterine gland cells and the degree of uterine glands folding were significantly increased in PE compared with NE. The uterus deformation included histological atrophy and fibrosis, which could lead to inadequate secretion of UF (Park and Sohn, 2018). Cui et al. suggested that such changes in the uterine glands stimulate the UF, increasing the content of Ca^{2+} for eggshell formation and affecting the eggshell quality (Cui et al., 2021). In brief, the formation of PE is associated with changes in the uterine glands. Another study reported that the morphological structure of the uterus determines the eggshell quality (Huntley and Holder, 1978). However, the molecular mechanism regulating the formation of pimpled eggshells has rarely been investigated.

MS-based proteomics is a powerful and versatile tool. Congjiao Sun et al. used proteomic analysis on eggshell matrix from strong and weak eggs and between the corresponding UFs. They identified 577 and 466 proteins in UF and eggshell matrix, respectively (Sun et al., 2013). Liu et al. identified 738 and 600 proteins in pimpled and normal calcified eggshells using label-free proteomics, respectively (Liu et al., 2017a). Here, we also used TMT-based quantitative proteomics technology to identify and quantify proteins in UFs from NE and PE hens. In total, 68 DAPs, including 24 upregulated and 44 downregulated proteins were identified in the PE group. Concerning the functional enrichment analysis, the DAPs were primarily related to 3 pathways: protein synthesis and folding, immune-related and cell growth and apoptosis.

The matrix protein regulating eggshell formation is a key factor affecting the quality of eggshells (Hernandez-Hernandez et al., 2008). In all cells, protein synthesis occurs at the ribosome. In the present study, we found that a 10 kDa heat shock protein (**HSPE1**) was upregulated, while the ribosomal protein L37 (**RPL37**), 60S ribosomal protein L35 (**RPL35**), and DnaJ homolog subfamily B member 6 (**DNAJB6**), 60S ribosomal protein L35a (**RPL35A**) were downregulated in the PE group compared to the NE group. HSPE1 together with Hsp60 participates in protein folding (Levy-Rimler et al., 2001). HSPE1 may be involved in endometrium changes during pregnancy (Forde et al., 2015). In addition, the downregulation of the Hspe1 gene was found to be associated with also reduced levels of proteins in other tissues (Christensen et al., 2010). DNAJB6, a co-chaperone with HSP70, helps in the folding of newly synthesized polypeptides and protein transport (Fernández-Fernández et al., 2017). DNAJB6 was also found in the eggshells, and we speculate that it plays an important role in the formation of eggshells. RPL37, RPL35, and RPL35A are the components of the 60S ribosomal subunit and participate in intracellular protein synthesis (Odintsova et al., 2003). RPL35 promotes the

proliferation of epithelial cells by regulating the synthesis of related proteins (Dai et al., 2021). However, the function of HSPE1, RPL37, RPL35, and RPL35A in avian species remains unclear, requiring further research. We can speculate that they may facilitate the formation of pimpled eggshells by affecting the synthesis and folding of related matrix proteins.

Moreover, we identified some DAPs related to the immune process including prohibitin1 (**PHB1**) and translin (**TSN**). Previous studies have found that disease or vaccination gives rise to the production of pimpled eggs (Broadfoot and Smith, 1954). Another study showed that the formation of eggshell abnormalities is associated with an immune response (Nii et al., 2014). PHB1 is a highly conserved protein and its downregulation leads to inflammatory responses (Liu et al., 2022). PHB1 regulates IgG1 levels in the plasma membrane by mediating CD86 signaling in B lymphocytes (Lucas et al., 2013). TSN, a DNA-binding protein, mostly binds to Ig/T-cell receptor gene segments (Aoki et al., 1997). In chicken oviducts, Ig is mainly distributed in the epithelial and glandular cells, and participates in local immune response (Kimijima et al., 1990). Feng et al. found that uterine inflammation inhibits calcium transport and matrix protein synthesis (Feng et al., 2023). In brief, we extrapolated that PHB1 and TSN may affect eggshell formation by regulating immune responses. Finally, there were some DAPs related to ion transport including calmodulin-1 (**CALM1**) and amiloride-sensitive sodium channel subunit gamma (**SCNN1G**) that were downregulated in the PE group. Ion transport plays an essential role in eggshell formation. Calcium participates in many physiological activities, and is a main component of eggshells (Eastin and Spaziani, 1978). CALM1, a calcium-binding protein, along with calcium ion channels regulates egg production (Reichow et al., 2013; Guo et al., 2023). CALM1 belongs to the EF-hand family of calcium-binding proteins, and with 4 EF domains, it can bind 4 calcium ions (Chen et al., 2015). Upon binding to calcium ions, its conformation changes, activating the downstream calmodulin-dependent protein kinase or phosphorylase that regulates intracellular calcium concentration (Bonnefond et al., 2015). CALM1 after binding to Ca^{2+} changes conformation, activating or inhibiting Ca^{2+} channels and PMCA receptors (Boczek et al., 2017). In addition, CALM1 may also have indirect, regulation by interacting with the regulators of Gprotein signaling in a Ca^{2+}-dependent manner, inducing calcium release (Popov et al., 2000). Especially, CALM1 can sense intracellular calcium levels and regulate calcium ion transport in uterine epithelial cells. CALM1 can play a crucial role in the formation of pimpled eggs (Liu et al., 2017a). Furthermore, during the eggshell formation, Na^{+} transport can also affect eggshell quality, especially the eggshell strength and thickness (Fan et al., 2013). Amiloride-sensitive Na^{+} channels are essential for the regulation of Na^{+} transport across epithelia (Benos and Stanton, 1999). SCNN1G, a member of the SCNN1 gene family, was found highly expressed in the uterus during eggshell deposition (Fan et al., 2013). Thus, we suggest that decreased expression of these proteins might affect ion transport in the uterus, inducing the production of pimpled eggs.

CONCLUSIONS

In summary, this demonstrated that the eggshell quality of NE was superior to PE. The uterus structure in PE hens promoted the formation of PE. The DAPs, such as CALM1, in the UF of PE hens may be associated with the formation of PE. These new findings may provide novel insights into the mechanism of PE production with potential applications for improving eggshell quality.

ACKNOWLEDGMENTS

The authors thank BioNovoGene (Suzhou, China) for technology support.

Funding: This work was financially supported by the earmarked fund for Jiangsu Agricultural Industry Technology System (Grant No. JATS[2022]163), and the Jiangsu Agriculture Independent Innovation (Grant No. CX(22)3033).

DISCLOSURES

The authors declare that they have no competing interests.

SUPPLEMENTARY MATERIALS

Supplementary material associated with this article can be found in the online version at doi:10.1016/j.psj.2023.103081.

REFERENCES

Ahmed, T. A. E., M. Younes, L. Wu, and M. T. Hincke. 2021. A survey of recent patents in engineering technology for the screening, separation and processing of eggshell. Front. Bioeng. Biotechnol. 9:677559.

Aoki, K., J. Inazawa, T. Takahashi, K. Nakahara, and M. Kasai. 1997. Genomic structure and chromosomal localization of the gene encoding translin, a recombination hotspot binding protein. Genomics 43:237–241.

Ashburner, M., C. A. Ball, J. A. Blake, D. Botstein, H. Butler, J. M. Cherry, A. P. Davis, K. Dolinski, S. S. Dwight, J. T. Eppig, M. A. Harris, D. P. Hill, L. Issel-Tarver, A. Kasarskis, S. Lewis, J. C. Matese, J. E. Richardson, M. Ringwald, G. M. Rubin, and G. Sherlock. 2000. Gene ontology: tool for the unification of biology. The Gene Ontology Consortium. Nat. Genet. 25:25–29.

Athanasiadou, D., W. Jiang, D. Goldbaum, A. Saleem, K. Basu, M. S. Pacella, C. F. Böhm, R. R. Chromik, M. T. Hincke, A. B. Rodríguez-Navarro, H. Vali, S. E. Wolf, J. J. Gray, K. H. Bui, and M. D. McKee. 2018. Nanostructure, osteopontin, and mechanical properties of calcitic avian eggshell. Sci. Adv. 4: eaar3219.

Benos, D. J., and B. A. Stanton. 1999. Functional domains within the degenerin/epithelial sodium channel (Deg/ENaC) superfamily of ion channels. J. Physiol. 520(Pt 3):631–644.

Boczek, T., M. Lisek, B. Ferenc, and L. Zylinska. 2017. Cross talk among PMCA, calcineurin and NFAT transcription factors in

control of calmodulin gene expression in differentiating PC12 cells. Biochim. Biophys. Acta. Gene Regul. Mech. 1860:502–515.
Bonnefond, M. L., B. Lambert, F. Giffard, E. Abeilard, E. Brotin, M. H. Louis, M. S. Gueye, P. Gauduchon, L. Poulain, and M. N'Diaye. 2015. Calcium signals inhibition sensitizes ovarian carcinoma cells to anti-Bcl-xL strategies through Mcl-1 down-regulation. Apoptosis 20:535–550.
Brionne, A., Y. Nys, C. Hennequet-Antier, and J. Gautron. 2014. Hen uterine gene expression profiling during eggshell formation reveals putative proteins involved in the supply of minerals or in the shell mineralization process. BMC Genom. 15:220.
Broadfoot, D. I., and W. M. Smith. 1954. Effects of infectious bronchitis in laying hens on egg production, percent unsettable eggs and hatchability. Poult. Sci. 33:653–654.
Chen, J., L. Li, Y. Li, X. Liang, Q. Sun, H. Yu, J. Zhong, Y. Ni, J. Chen, Z. Zhao, P. Gao, B. Wang, D. Liu, Z. Zhu, and Z. Yan. 2015. Activation of TRPV1 channel by dietary capsaicin improves visceral fat remodeling through connexin43-mediated Ca^{2+} influx. Cardiovasc. Diabetol. 14:22.
Cheng, X., and Z. Ning. 2023. Research progress on bird eggshell quality defects: a review. Poult. Sci. 102:102283.
Christensen, J. H., M. N. Nielsen, J. Hansen, A. Füchtbauer, E. M. Füchtbauer, M. West, T. J. Corydon, N. Gregersen, and P. Bross. 2010. Inactivation of the hereditary spastic paraplegia-associated Hspd1 gene encoding the Hsp60 chaperone results in early embryonic lethality in mice. Cell Stress Chaperones 15:851–863.
Cui, Z., Z. Zhang, F. K. Amevor, X. Du, L. Li, Y. Tian, X. Kang, G. Shu, Q. Zhu, Y. Wang, D. Li, Y. Zhang, and X. Zhao. 2021. Circadian miR-449c-5p regulates uterine Ca^{2+} transport during eggshell calcification in chickens. BMC Genom. 22:764.
Dai, P., X. Deng, P. Liu, L. Li, D. Luo, Y. Liao, and Y. Zeng. 2021. Mycoplasma genitalium protein of adhesion promotes the early proliferation of human urothelial cells by interacting with RPL35. Pathogens 10:1449.
Dunn, I. C., A. B. Rodríguez-Navarro, K. McDade, M. Schmutz, R. Preisinger, D. Waddington, P. W. Wilson, and M. M. Bain. 2012. Genetic variation in eggshell crystal size and orientation is large and these traits are correlated with shell thickness and are associated with eggshell matrix protein markers. Anim. Genet. 43:410–418.
Eastin, W. C. Jr., and E. Spaziani. 1978. On the control of calcium secretion in the avian shell gland (uterus). Biol. Reprod. 19:493–504.
Ebeid, T. A., T. Suzuki, and T. Sugiyama. 2012. High ambient temperature influences eggshell quality and calbindin-D28k localization of eggshell gland and all intestinal segments of laying hens. Poult. Sci. 91:2282–2287.
Fan, Y. F., Z. C. Hou, G. Q. Yi, G. Y. Xu, and N. Yang. 2013. The sodium channel gene family is specifically expressed in hen uterus and associated with eggshell quality traits. BMC Genet. 14:90.
Feng, J., M. Lu, L. Ma, H. Zhang, S. Wu, K. Qiu, Y. Min, G. Qi, and J. Wang. 2023. Uterine inflammation status modulates eggshell mineralization via calcium transport and matrix protein synthesis in laying hens. Anim. Nutr. 13:411–425.
Fernández-Fernández, M. R., M. Gragera, L. Ochoa-Ibarrola, L. Quintana-Gallardo, and J. M. Valpuesta. 2017. Hsp70 − a master regulator in protein degradation. FEBS Lett. 591:2648–2660.
Forde, N., F. W. Bazer, T. E. Spencer, and P. Lonergan. 2015. 'Conceptualizing' the endometrium: identification of conceptus-derived proteins during early pregnancy in cattle. Biol. Reprod. 92:156.
Fu, K., D. Zheng, Z. Xiao, Y. Chen, L. Wang, S. Lian, A. Li, and X. Wu. 2023. Correlations between organic matrix and eggshell properties of 3 kinds of eggshells in Muscovy duck (Cairina moschata). Poult. Sci. 102:102836.
Gongruttananun, N. 2018. Induced molt using cassava meal. 2. Effects on eggshell quality, ultrastructure, and pore density in late-phase laying hens. Poult. Sci. 97:1050–1058.
Guo, S., Y. Bai, Q. Zhang, H. Zhang, Y. Fan, H. Han, and Y. Liu. 2023. Associations of CALM1 and DRD1 polymorphisms, and their expression levels, with Taihang chicken egg-production traits. Anim. Biotechnol. 34:994–1004.
Hahn, E. N., V. R. Sherman, A. Pissarenko, S. D. Rohrbach, D. J. Fernandes, and M. A. Meyers. 2017. Nature's technical ceramic: the avian eggshell. J. R. Soc. Interface 14:20160804.
Hernandez-Hernandez, A., J. Gomez-Morales, A. B. Rodriguez-Navarro, J. Gautron, Y. Nys, and J. M. García-Ruiz. 2008. Identification of some active proteins in the process of hen eggshell formation. Cryst. Growth Des. 8:4330–4339.
Hincke, M. T., Y. Nys, J. Gautron, K. Mann, A. B. Rodriguez-Navarro, and M. D. McKee. 2012. The eggshell: structure, composition and mineralization. Front. Biosci. (Landmark Ed.) 17:1266–1280.
Huntley, D. M., and D. P. Holder. 1978. Ultrastructure of shell gland tissue from hens producing good and poor eggshells. Poult. Sci. 57:1365–1368.
Kanehisa, M., S. Goto, S. Kawashima, Y. Okuno, and M. Hattori. 2004. The KEGG resource for deciphering the genome. Nucleic Acids Res. 32:D277–D280.
Kimijima, T., Y. Hashimoto, H. Kitagawa, Y. Kon, and M. Sugimura. 1990. Localization of immunoglobulins in the chicken oviduct. Nihon. Juigaku. Zasshi. 52:299–305.
Levy-Rimler, G., P. Viitanen, C. Weiss, R. Sharkia, A. Greenberg, A. Niv, A. Lustig, Y. Delarea, and A. Azem. 2001. The effect of nucleotides and mitochondrial chaperonin 10 on the structure and chaperone activity of mitochondrial chaperonin 60. Eur. J. Biochem. 268:3465–3472.
Liu, H., H. Fan, P. He, H. Zhuang, X. Liu, M. Chen, W. Zhong, Y. Zhang, C. Zhen, Y. Li, H. Jiang, T. Meng, Y. Xu, G. Zhao, and D. Feng. 2022. Prohibitin 1 regulates mtDNA release and downstream inflammatory responses. EMBO J. 41:e111173.
Liu, Z., L. Song, L. Lu, X. Zhang, F. Zhang, K. Wang, and R. J. Linhardt. 2017a. Comparative proteomics of matrix fractions between pimpled and normal chicken eggshells. J. Proteom. 167:1–11.
Liu, Z., L. Song, F. Zhang, W. He, and R. J. Linhardt. 2017b. Characteristics of global organic matrix in normal and pimpled chicken eggshells. Poult. Sci. 96:3775–3784.
Lucas, C. R., H. M. Cordero-Nieves, R. S. Erbe, J. W. McAlees, S. Bhatia, R. J. Hodes, K. S. Campbell, and V. M. Sanders. 2013. Prohibitins and the cytoplasmic domain of CD86 cooperate to mediate CD86 signaling in B lymphocytes. J. Immunol. 190:723–736.
Marie, P., V. Labas, A. Brionne, G. Harichaux, C. Hennequet-Antier, Y. Nys, and J. Gautron. 2014. Data set for the proteomic inventory and quantitative analysis of chicken uterine fluid during eggshell biomineralization. Data Brief. 1:65–69.
Marie, P., V. Labas, A. Brionne, G. Harichaux, C. Hennequet-Antier, Y. Nys, and J. Gautron. 2015. Quantitative proteomics and bioinformatic analysis provide new insight into protein function during avian eggshell biomineralization. J. Proteom. 113:178–193.
Nii, T., N. Isobe, and Y. Yoshimura. 2014. Effects of avian infectious bronchitis virus antigen on eggshell formation and immunoreaction in hen oviduct. Theriogenology 81:1129–1138.
Nys, Y., J. Gautron, J. M. Garcia-Ruiz, and M. T. Hincke. 2004. Avian eggshell mineralization: biochemical and functional characterization of matrix proteins. C. R. Palevol. 3:549–562.
Nys, Y., M. T. Hincke, A. Hernandez-Hernandez, A. B. Rosriguez-Navarro, and J. Gautron. 2010. Eggshell ultrastructure, properties and the process of mineralization: involvement of organic matrix in the eggshell fabric. INRA Product. Anim. 23:143–154.
Odintsova, T. I., E. C. Müller, A. V. Ivanov, T. A. Egorov, R. Bienert, S. N. Vladimirov, S. Kostka, A. Otto, B. Wittmann-Liebold, and G. G. Karpova. 2003. Characterization and analysis of posttranslational modifications of the human large cytoplasmic ribosomal subunit proteins by mass spectrometry and Edman sequencing. J. Protein Chem. 22:249–258.
Pan, X. F., J. J. Yang, L. P. Lipworth, X. O. Shu, H. Cai, M. D. Steinwandel, W. J. Blot, W. Zheng, and D. Yu. 2021. Cholesterol and egg intakes with cardiometabolic and all-cause mortality among Chinese and low-income Black and White Americans. Nutrients 13:2094.
Park, J. A., and S. H. Sohn. 2018. The influence of hen aging on eggshell ultrastructure and shell mineral components. Korean J. Food Sci. Anim. Resour. 38:1080–1091.
Popov, S. G., U. M. Krishna, J. R. Falck, and T. M. Wilkie. 2000. Ca^{2+}/calmodulin reverses phosphatidylinositol 3,4, 5-trisphosphate-dependent inhibition of regulators of G protein-signaling GTPase-activating protein activity. J. Biol. Chem. 275:18962–18968.

Radwan, L. M. 2015. Eggshell quality: a comparison between Fayoumi, Gimieizah and Brown Hy-Line strains for mechanical properties and ultrastructure of their eggshells. Anim. Prod. Sci. 56:908–912.

Reichow, S. L., D. M. Clemens, J. A. Freites, K. L. Németh-Cahalan, M. Heyden, D. J. Tobias, J. E. Hall, and T. Gonen. 2013. Allosteric mechanism of water-channel gating by Ca^{2+}-calmodulin. Nat. Struct. Mol. Biol. 20:1085–1092.

Rodriguez-Navarro, A., O. Kalin, Y. Nys, and J. M. Garcia-Ruiz. 2002. Influence of the microstructure on the shell strength of eggs laid by hens of different ages. Br. Poult. Sci. 43:395–403.

Roland Sr, D., J. Thompson, R. Voitle, and R. Harms. 1975. Studies on the cause, prevention and artificial creation of pimpled egg shells. Poult. Sci. 54:1485–1491.

Subramanian, A., P. Tamayo, V. K. Mootha, S. Mukherjee, B. L. Ebert, M. A. Gillette, A. Paulovich, S. L. Pomeroy, T. R. Golub, E. S. Lander, and J. P. Mesirov. 2005. Gene set enrichment analysis: a knowledge-based approach for interpreting genome-wide expression profiles. Proc. Natl. Acad Sci. U S A 102:15545–15550.

Sun, C., G. Xu, and N. Yang. 2013. Differential label-free quantitative proteomic analysis of avian eggshell matrix and uterine fluid proteins associated with eggshell mechanical property. Proteomics 13:3523–3536.

Szklarczyk, D., A. L. Gable, D. Lyon, A. Junge, S. Wyder, J. Huerta-Cepas, M. Simonovic, N. T. Doncheva, J. H. Morris, P. Bork, L. J. Jensen, and C. V. Mering. 2019. STRING v11: protein-protein association networks with increased coverage, supporting functional discovery in genome-wide experimental datasets. Nucleic Acids Res. 47:D607–D613.

Van Toledo, B., A. H. Parsons, and G. F. Combs. 1982. Role of ultrastructure in determining eggshell strength. Poult. Sci. 61:569–572.

Wang, X., P. Zhu, Z. Sun, J. Zhang, and C. Sun. 2021. Uterine metabolomic analysis for the regulation of eggshell calcification in chickens. Metabolites 11:575.

Wasserman, R. H., C. A. Smith, C. M. Smith, M. E. Brindak, C. S. Fullmer, L. Krook, J. T. Penniston, and R. Kumar. 1991. Immunohistochemical localization of a calcium pump and calbindin-D28k in the oviduct of the laying hen. Histochemistry 96:413–418.

Wiśniewski, J. R., A. Zougman, N. Nagaraj, and M. Mann. 2009. Universal sample preparation method for proteome analysis. Nat. Methods 6:359–362.

Wolc, A., J. Arango, P. Settar, N. P. O'Sullivan, V. E. Olori, I. M. White, W. G. Hill, and J. C. Dekkers. 2012. Genetic parameters of egg defects and egg quality in layer chickens. Poult. Sci. 91:1292–1298.

Woudstra, T., and A. B. Thomson. 2002. Nutrient absorption and intestinal adaptation with ageing. Best Pract. Res. Clin. Gastroenterol. 16:1–15.

Zhang, Y., F. Jiang, B. Yang, S. Wang, H. Wang, A. Wang, D. Xu, and W. Fan. 2022. Improved microbial genomes and gene catalog of the chicken gut from metagenomic sequencing of high-fidelity long reads. Gigascience 11:giac116.

Zhang, J., Y. Wang, C. Zhang, M. Xiong, S. A. Rajput, Y. Liu, and D. Qi. 2019. The differences of gonadal hormones and uterine transcriptome during shell calcification of hens laying hard or weak-shelled eggs. BMC Genom. 20:707.

Zhang, Y. N., H. J. Zhang, S. G. Wu, J. Wang, and G. H. Qi. 2017. Dietary manganese supplementation modulated mechanical and ultrastructural changes during eggshell formation in laying hens. Poult. Sci. 96:2699–2707.

Zhu, M., H. Li, L. Miao, L. Li, X. Dong, and X. Zou. 2020. Dietary cadmium chloride impairs shell biomineralization by disrupting the metabolism of the eggshell gland in laying hens. J. Anim. Sci. 98 skaa025.

Zhu, F., F. Zhang, M. Hincke, Z. T. Yin, S. R. Chen, N. Yang, and Z. C. Hou. 2019. iTRAQ-based quantitative proteomic analysis of duck eggshell during biomineralization. Proteomics 19:e1900011.